

## Synthesis and evaluation of novel 3,4,6-substituted 2-quinolones as FMS kinase inhibitors

Mark J. Wall, Jinsheng Chen, Sanath Meegalla, Shelley K. Ballentine, Kenneth J. Wilson, Renee L. DesJarlais, Carsten Schubert, Margery A. Chaikin, Carl Crysler, Ioanna P. Petrounia, Robert R. Donatelli, Edward J. Yurkow, Lisa Boczon, Marie Mazzulla, Mark R. Player, Raymond J. Patch, Carl L. Manthey, Christopher Molloy, Bruce Tomczuk and Carl R. Illig\*

*Johnson & Johnson Pharmaceutical Research & Development, Welsh & McKean Roads, Spring House, PA 19477, USA*

Received 14 December 2007; revised 21 January 2008; accepted 23 January 2008

Available online 30 January 2008

**Abstract**—A series of 3,4,6-substituted 2-quinolones has been synthesized and evaluated as inhibitors of the kinase domain of macrophage colony-stimulating factor-1 receptor (FMS). The fully optimized compound, 4-(4-ethyl-phenyl)-3-(2-methyl-3*H*-imidazol-4-yl)-2-quinolone-6-carbonitrile **21b**, has an  $IC_{50}$  of 2.5 nM in an in vitro assay and 5.0 nM in a bone marrow-derived macrophage cellular assay. Inhibition of FMS signaling in vivo was also demonstrated in a mouse pharmacodynamic model.

© 2008 Elsevier Ltd. All rights reserved.

The macrophage colony-stimulating factor-1 receptor (FMS) is the cell surface receptor for colony-stimulating factor-1 (CSF-1), which controls growth and differentiation of the monocyte/macrophage lineage.<sup>1</sup> FMS is a member of the type III receptor tyrosine kinases that also includes FLT-3, PDGFR, and KIT. Macrophages are thought to play an important role in several diseases, including cancer and inflammation. For example, of the several leukocyte lineages present in the rheumatoid arthritis synovium, increased levels of macrophages best correlate with disease severity and response to therapy.<sup>2</sup> In addition, expression of FMS in breast cancer has been linked to poor survivability and increased tumor size, where presumably the receptor is involved in local invasion and metastasis.<sup>3–5</sup> Consequently there is significant interest in modulating the CSF-1 pathway and several structural classes of small-molecule inhibitors of FMS have been reported.<sup>6–11</sup>

We have recently published an X-ray crystal structure of the FMS kinase domain in complex with two classes of

inhibitors.<sup>11</sup> In this paper we describe the synthesis and optimization of one of these classes of compounds, the 2-quinolones, shown in Figure 1.

A high-throughput screen using Thermofluor<sup>®</sup> technology<sup>12</sup> produced quinolone **1**, with an  $IC_{50}$  of 1  $\mu$ M for FMS. Initial chemistry efforts began by synthesizing analogues with substitution in the 3- and 6-positions of the quinolone. These compounds could be readily prepared by condensation of 2-aminophenyl ketones **2** with  $\alpha$ -substituted acetic acids in phosphorus oxychloride to give the corresponding 2-chloroquinolones **3** that are subsequently hydrolyzed to the corresponding quinolones **4** in aqueous acetic acid according to the procedures outlined in Scheme 1. The aminophenyl ketones

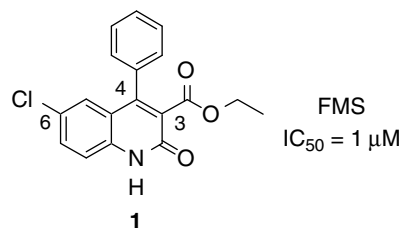
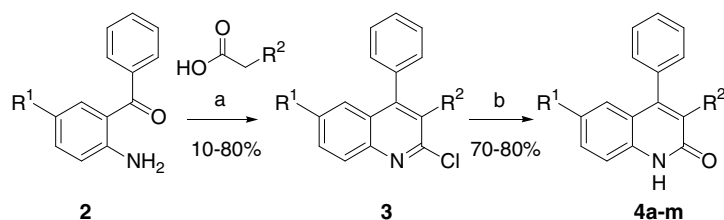


**Figure 1.** Thermofluor<sup>®</sup> HTS screening hit.

**Keywords:** FMS; cFMS; Colony-stimulating factor-1 receptor; CSF-1; M-CSF; 2-Quinolones.

\* Corresponding author. Tel.: +1 610 458 6057; fax: +1 610 458 8249; e-mail: [cillig@prdus.jnj.com](mailto:cillig@prdus.jnj.com)



**Scheme 1.** Reagents and conditions: (a) Phosphorus oxychloride, 105 °C; (b) 80% aqueous acetic acid, ammonium acetate, 110 °C.

and acetic acids used were commercially available, with the exception of the 5-cyano analogue of **2** that was prepared from the 5-bromo compound by reaction with CuCN in refluxing DMF. Initial SAR studies probed substituent effects at the 3-position of the quinolone. Ethyl, methyl, and isopropyl esters for  $R_2$  were found to be equipotent, whereas activity diminished with more sterically demanding esters. The direct 3-ethylamido analogue ( $R_2 = \text{CONHEt}$ ) was inactive, as was the corresponding free carboxylic acid (data not shown). However, a variety of five-membered aromatic heterocycles were identified as suitable replacements for the ethyl carboxylate (Table 1). Of these, 3-methylisoxazol-5-yl was the most potent providing a 7-fold improvement over the original hit compound (compare **4a** to **1**). More basic aromatic heterocycles such as imidazole **4k** also afforded a significant (5-fold) increase in potency relative to **1**.

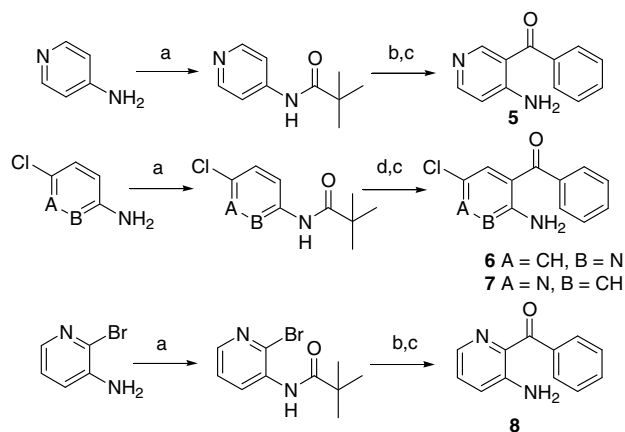
The importance of substitution at the 6-position of the quinolone system was demonstrated in early series analogues. A dramatic loss of activity (>50-fold) was observed with the des-chloro analogue of **1**; the 7- and 8-positional isomers were also found to be inactive (data not shown). Additional studies probing substituent effects at the 6-position were carried out on 3-isoxazol-5-yl analogues (Table 1). In this case, chloro and cyano groups (**4a** and **4b**, respectively) imparted the highest levels of activity.

The SAR of the central core of the quinolone scaffold was examined next by preparing the 1,8-, 1,7-, 1,6-, and 1,5-naphthyridin-2-one analogues (**9a–d**). The synthesis of these compounds required aminopyridyl ketones **5–8** that were synthesized according to the procedures outlined in Scheme 2. Compounds **5–7** were prepared according to the procedure of Turner<sup>14</sup> by ortho lithiation of 2-, 3-, and 4-(pivaloylamino)pyridines followed by quenching with the Weinreb amide<sup>15</sup> of benzoic acid and acid-catalyzed removal of the pivaloyl group. The 3-aminopyridyl-2-phenyl ketone **8** was prepared by lithium-bromine exchange of 2-bromo-3-(pivaloylamino)pyridine followed by quenching with the Weinreb amide and deprotection. The aminopyridyl ketones **5–8** were then condensed with 3-methylisoxazole-5-acetic acid according to the procedures in Scheme 1 to give compounds **9a–d**.

The most potent compound was the 1,7-naphthyridin-2-one **9b** (Table 2), which was 5-fold less potent than the analogous quinolone compound **4a**. The 1,8-naphthyridin-2-one **9a** also had some activity ( $\text{IC}_{50} = 1 \mu\text{M}$ ), but,

**Table 1.** FMS kinase activity of compounds **4a–m**<sup>13</sup>

Compound	$R^1$	$R^2$	$\text{IC}_{50}$ ( $\mu\text{M}$ )
<b>4a</b>	Cl		0.14
<b>4b</b>	CN		0.09
<b>4c</b>	F		0.25
<b>4d</b>	$\text{NO}_2$		0.34
<b>4e</b>	$\text{NH}_2$		>5
<b>4f</b>	H		>5
<b>4g</b>	Cl		0.30
<b>4h</b>	Cl		0.32
<b>4i</b>	Cl		0.36
<b>4j</b>	Cl		0.83
<b>4k</b>	Cl		0.18
<b>4l</b>	CN		0.28
<b>4m</b>	CN		0.55



**Scheme 2.** Reagents and conditions: (a) Pivaloyl chloride,  $\text{NEt}_3$ , DCM; (b)  $n\text{-BuLi}$ , THF,  $-78^\circ\text{C}$ , 3 h, then PhCONMeOMe; (c) 3 N HCl,  $100^\circ\text{C}$ ; (d)  $t\text{-BuLi}$ , THF,  $-78^\circ\text{C}$ , 3 h, then PhCONMeOMe.

**Table 2.** FMS kinase activity of naphthyridones **9a–d**

Compound	Structure	$\text{IC}_{50}$ ( $\mu\text{M}$ )
<b>9a</b>		1.0
<b>9b</b>		0.72
<b>9c</b>		8% <sup>a</sup>
<b>9d</b>		>20

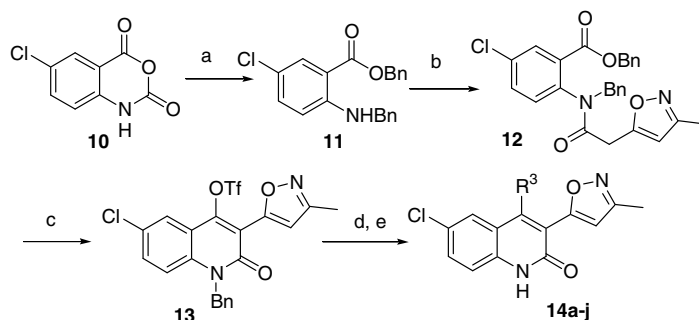
<sup>a</sup> Percent inhibition at 5  $\mu\text{M}$ .

in general, these compounds were less active and this scaffold was not further investigated.

The synthetic route used to optimize the 4-substituent is shown in **Scheme 3**. Since few aminophenylketones **2** were commercially available, an alternate synthetic route to our earlier method (**Scheme 1**) was required. Thus, 5-chloroisatoic anhydride **10** was first converted to the dibenzyl-protected aminobenzoate **11**, which was then coupled to 3-methylisoxazole-5-acetic acid using neat phosphorus oxychloride. Cyclization with NaH, followed by reaction with triflic anhydride gave the triflate **13**. The triflate was then coupled to boronic acids using a Suzuki–Miyaura reaction, followed by benzyl deprotection with neat triflic acid to yield compounds **14a–j**.

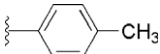
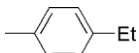
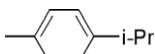
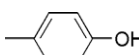
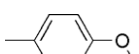
The data in **Table 3** show that only a modest 1.5-fold improvement in potency over the unsubstituted phenyl group was obtained with a 4-ethylphenyl group **14b** or with a cycloheptene ring **14g**. With the former, ethyl substitution appears to be optimal; methyl and isopropyl substitution resulted in diminished activity. Within the cycloalkene series, the cycloheptene **14g** was more potent than the cyclohexene **14f** (>2-fold), and saturation to the cyclohexane **14h** further reduced activity. We attempted to introduce polar functionality in this portion of the molecule to improve the solubility and potency of the series. Hydroxy and methoxy substituents (**14d** and **14e**, respectively), while tolerated, afforded no increase in inhibitory potency. Conversely, incorporation of a pyridyl ring (**14i**) significantly attenuated activity.

In the course of these analogue studies, an X-ray crystal structure of quinolone **4a** bound to the FMS kinase domain was obtained.<sup>11</sup> **Figure 2** shows compound **4a** bound in the nucleotide-binding pocket of FMS in the inactive form. Both the N-1 and O-2 of the quinolone ring, in the keto tautomeric form, make hydrogen bonds with the backbone of the hinge residues Cys666 (2.90 Å) and Glu664 (3.32 Å). The hydrophobic phenyl ring occupies the ribose-binding pocket, and the chloroaryl ring is located in the adenine pocket. The 3-methylisoxazole is rotationally disordered. Two positions are seen which differ by a 180-degree rotation of the bond with the quinolone core. Specific interactions between the 3-methylisoxazole and the protein are not observed.



**Scheme 3.** Reagents and conditions: (a) Benzyl bromide,  $\text{Na}_2\text{CO}_3$ , DMF; (b) 3-methylisoxazole-5-acetic acid, phosphorus oxychloride; (c) NaH, triflic anhydride, DMF; (d)  $\text{R}_3\text{B}(\text{OH})_2$ ,  $\text{Pd}(\text{PPh}_3)_4$ ,  $\text{Na}_2\text{CO}_3$ , toluene, ethanol,  $80^\circ\text{C}$ ; (e) triflic acid.

**Table 3.** FMS kinase activity of compounds **14a–j**

Compound	R <sup>3</sup>	IC <sub>50</sub> (μM)
<b>14a</b>		0.11
<b>14b</b>		0.09
<b>14c</b>		0.20
<b>14d</b>		0.17
<b>14e</b>		0.14
<b>14f</b>		0.22
<b>14g</b>		0.09
<b>14h</b>		0.34
<b>14i</b>		2.1
<b>14j</b>		0.24

In light of this structural information, we re-visited quinolone analogues substituted at the 3-position with imidazole systems, as these generally tended to exhibit improved solubility characteristics as compared with their isoxazole counterparts. Specifically, we targeted 2-methylimidazole derivatives, since these were expected to occupy the same spatial region as the 3-methylisoxazole system in this protein-binding mode.

The synthesis of the required 2-methylimidazole-5-acetic acid **17** is shown in Scheme 4. 2-Methylimidazole was protected with a SEM group, which directs the metallation with *tert*-butyl lithium to imidazole C-5. The anion was quenched with *N,N*-dimethylformamide to yield the aldehyde **16**, which was subsequently homologated to the acetic acid ethyl ester using methyl (methylthio)methyl sulfoxide followed by ethanolic HCl.<sup>16</sup> The ester was then hydrolyzed to the acid using KOH to give **17**. We then prepared aminoketones **20a,b** to incorporate the optimized groups in the C-4 and C-6 positions of the quinolone scaffold. This was accomplished from

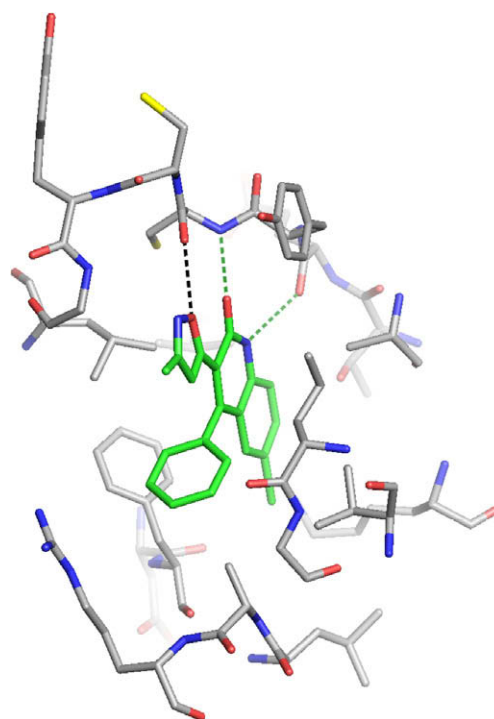
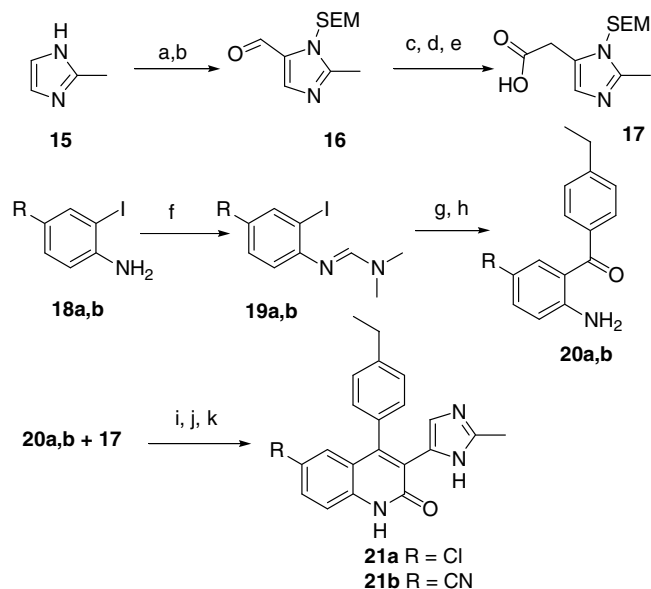


**Figure 2.** Crystal structure of **4a** bound to the FMS kinase domain. FMS residues within 5 Å of the quinolone are shown with gray carbons and the quinolone is shown with green carbons. The green dotted lines represent hydrogen bonds made by the quinolone core. The black dotted line is a close contact between two oxygens in the structure and predicted hydrogen bonds for the imidazoles **21a** and **21b**. (PDB Id: 2i0v).



**Scheme 4.** Reagents and conditions: (a) SEMCl, NaH, DMF; (b) *t*-BuLi, DMF, THF, −78 °C; (c) MeSCH<sub>2</sub>SOMe, NaH, THF; (d) 3 N HCl (g)/EtOH; (e) 2 N KOH, ethanol; (f) DMF dimethyl acetal, toluene, 100 °C; (g) *i*-PrMgCl, 4-EtPhCONMeOMe; (h) 3 N aq HCl, THF; (i) POCl<sub>3</sub>, DCM, 25 °C; (j) piperidine, toluene, 110 °C; (k) 6 N HCl (aqueous), ethanol (1:1), 80 °C.

the 4-chloro- or 4-cyano-2-iodoaniline by first protecting the amino group as the amidine followed by formation of the Grignard reagent with isopropylmagnesium

**Table 4.** IC<sub>50</sub> data for compounds **21a,b** for cellular BMDM FMS assay and for in vitro FMS, FLT-3, KIT, and PDGFR- $\beta$  assays

Compound	BMDM ( $\mu$ M)	FMS ( $\mu$ M)	FLT-3 ( $\mu$ M)	KIT ( $\mu$ M)	PDGFR- $\beta$ ( $\mu$ M)
<b>21a</b>	0.028	0.0021	0.034	0.067	>1
<b>21b</b>	0.005	0.0025	0.047	0.170	>1

**Table 5.** Pharmacokinetic parameters for **21b** in rat; 2 mg/kg IV and 10 mg/kg PO

Compound	<i>t</i> <sub>1/2</sub> (IV) (min)	C <sub>max</sub> (ng/ml)	V <sub>Z</sub> (ml/kg)	Cl (ml/min/kg)	F (%)
21b	64	317	8600	93	56

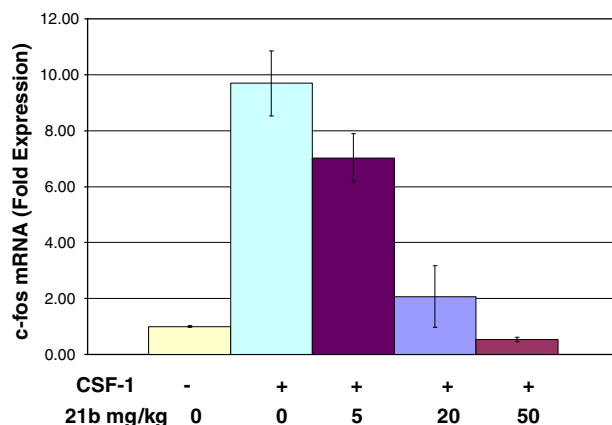
chloride according to the method of Knochel.<sup>17,18</sup> The magnesium species was then reacted with the Weinreb amide of 4-ethylbenzoic acid followed by amidine deprotection to give **20a,b**. The aminophenylketones **20a,b** were then coupled to the imidazole acetic acid **17** with phosphorus oxychloride in dichloromethane followed by cyclization with piperidine in refluxing toluene. Finally, SEM group removal was effected with 6 N HCl in ethanol to give **21a,b**.

The data in Table 4 show that introduction of a 2-methyl group on the imidazole has a profound effect on the activity of the series. In the enzymatic assay, both compounds were in the 2 nM range and, in the cellular assay that measures proliferation of bone marrow-derived macrophages (BMDM)<sup>10</sup> in response to CSF-1, the cyano **21b** was 5 nM, 5-fold better than the chloro **21a**. It appears that the imidazole can make an additional hydrogen bond with the FMS kinase (see Fig. 2). This may be the reason for the improved activity of the imidazole compared to the isoxazole. There is no clear structural explanation for the large gain in activity with the addition of the methyl group.

The selectivity of **21a** and **21b** toward other kinases in the type III receptor kinase family (FLT-3, KIT, and PDGFR- $\beta$ ) was also evaluated (Table 4).<sup>13</sup> Both compounds showed excellent selectivity for FMS versus PDGFR- $\beta$  (>400-fold) and, versus KIT, good selectivity was also achieved (70- and 30-fold for cyano and chloro analogues **21b** and **21a**, respectively). Both compounds exhibited modest selectivity for FMS versus FLT-3, (15- to 20-fold).

The pharmacokinetic profile of compound **21b** in the rat shows that the compound has good oral bioavailability at 56% (Table 5), although the rate of clearance was high.

Having obtained suitable pharmacokinetics for in vivo testing, compound **21b** was evaluated in a mouse pharmacodynamic model that is based on the ability of CSF-1 to induce c-fos mRNA in macrophages.<sup>19</sup> Following tail vein injection of CSF-1, c-fos mRNA increased more than 10-fold in the spleen. The induction was robust within 15 min but was transient, returning

**Figure 3.** Pharmacodynamic activity of **21b** at FMS. B6C3F1 mice were dosed orally with **21b** in 20% 2-hydroxypropyl- $\beta$ -cyclodextrin and 6 h later given an iv injection containing 1.0  $\mu$ g recombinant CSF-1. Fifteen minutes later, the mice were euthanized and c-fos mRNA was measured in spleen lysates.

to baseline by 30 min. Furthermore, this induced expression was shown to be dose-dependent and specific for CSF-1 as it was blocked completely in mice pre-dosed with anti-CSF-1 (data not shown). Figure 3 shows the FMS inhibitory effect of an oral dose of 5, 20, and 50 mg/kg of **21b** after 6 h. In the group treated with 50 mg/kg of **21b**, c-fos mRNA expression was reduced to control levels showing that FMS signaling is completely inhibited.

In conclusion, we have identified a novel and potent class of FMS kinase inhibitors based on a quinolone core. The compounds have good selectivity versus highly homologous kinases and good oral bioavailability. Inhibition of FMS signaling in vivo was also demonstrated in a mouse pharmacodynamic model.

## References and notes

- Sherr, C. J. *Biochim. Biophys. Acta* **1988**, *948*, 225.
- Moss, S. T.; Hamilton, J. A. *Immunobiology* **2000**, *202*, 18.
- Kluger, H. M.; Dolled-Filhart, M.; Rodov, S.; Kacinski, B. M.; Camp, R. L.; Rimm, D. L. *Clin. Cancer Res.* **2004**, *10*, 173.
- Lin, E. Y.; Nguyen, A. V.; Russell, R. G.; Pollard, J. W. *J. Exp. Med.* **2001**, *193*, 727.
- Yee, L. D.; Liu, L. *Anticancer Res.* **2000**, *20*, 4379.
- Conway, J. G.; McDonald, B.; Parham, J.; Keith, B.; Rusnak, D. W.; Shaw, E.; Jansen, M.; Lin, P.; Payne, A.; Crosby, R. M.; Johnson, J. H.; Frick, L.; Lin, M. H.; Depee, S.; Tadepalli, S.; Votta, B.; James, I.; Fuller, K.; Chambers, T. J.; Kull, F. C.; Chamberlain, S. D.; Hutchins, J. T. *Proc. Natl. Acad. Sci. U.S.A.* **2005**, *102*, 16078.
- Irvine, K. M.; Burns, C. J.; Wilks, A. F.; Su, S.; Hume, D. A.; Sweet, M. J. *FASEB J.* **2006**, *20*, 1921.
- Ohno, H.; Kubo, K.; Murooka, H.; Kobayashi, Y.; Nishitoba, T.; Shibuya, M.; Yoneda, T.; Isoe, T. *Mol. Cancer Ther.* **2006**, *5*, 2634.
- Smalley, T. L., Jr.; Chamberlain, S. D.; Mills, W. Y.; Musso, D. L.; Randhawa, S. A.; Ray, J. A.; Samano, V.; Frick, L. *Bioorg. Med. Chem. Lett.* **2007**, *17*, 6257.

10. Patch, R. J.; Brandt, B. M.; Asgari, D.; Baidur, N.; Chadha, N. K.; Georgiadis, T.; Cheung, W. S.; Petrounia, I. P.; Donatelli, R. R.; Chaikin, M. A.; Player, M. R. *Bioorg. Med. Chem. Lett.* **2007**, *17*, 6070.
11. Schubert, C.; Schalk-Hihi, C.; Struble, G. T.; Ma, H. C.; Petrounia, I. P.; Brandt, B.; Deckman, I. C.; Patch, R. J.; Player, M. R.; Spurlino, J. C.; Springer, B. A. *J. Biol. Chem.* **2007**, *282*, 4094.
12. Carver, T. E.; Bordeau, B.; Cummings, M. D.; Petrella, E. C.; Pucci, M. J.; Zawadzke, L. E.; Dougherty, B. A.; Tredup, J. A.; Bryson, J. W.; Yanchunas, J., Jr.; Doyle, M. L.; Witmer, M. R.; Nelen, M. I.; DesJarlais, R. L.; Jaeger, E. P.; Devine, H.; Asel, E. D.; Springer, B. A.; Bone, R.; Salemme, F. R.; Todd, M. J. *J. Biol. Chem.* **2005**, *280*, 11704.
13. FMS, FLT-3, KIT, and PDGFR- $\beta$  kinase assays: The full cytoplasmic regions of FMS (538–972) and FLT-3 (571–993) encompassing the tyrosine kinase domains were expressed and purified from a baculovirus system as described (Schalk-Hihi, C.; Ma, H. C.; Struble, G. T.; Bayoumy, S.; Williams, R.; Devine, E.; Petrounia, I. P.; Mezzasalma, T.; Zeng, L.; Schubert, C.; Grasberger, B.; Springer, B. A.; Deckman, I. C. *J. Biol. Chem.* **2007**, *282*, 4085). KIT and PDGFR- $\beta$  was purchased from ProQinase. FMS 555–568 peptide (SYEGNSYTFIDPTQ) was synthesized and purified by AnaSpec. FMS was assayed using a fluorescence polarization (FP) competition immunoassay that measured FMS phosphorylation of FMS 555–568 peptide at Y561. The reaction mixture (10  $\mu$ L) contained 100 mM Hepes, pH 7.5, 1 mM DTT, 0.01% Tween 20 (v/v), 2% DMSO, 308  $\mu$ M FMS 555–568 peptide, 1 mM ATP, 5 mM MgCl<sub>2</sub>, and 0.7 nM FMS. The reaction was initiated with ATP, incubated 80 min at room temperature, and quenched by the addition of 5.4 mM EDTA. Ten microliters of FP buffer/tracer/phospho-Y antibody mix (Tyrosine kinase assay kit, Green P2837, Invitrogen) was added to the quenched reaction, and FP was measured after 30 min using an Analyst reader (Molecular Devices) at excitation/emission of 485/530 nm. FLT-3, KIT, and PDGFR- $\beta$  were assayed using the fluorescence polarization competition format as described for FMS except that poly Glu<sub>4</sub>Tyr (Sigma) was used as a universal substrate. FLT-3 reactions contained 10 nM FLT-3, 113  $\mu$ M ATP, and 20  $\mu$ g/ml poly Glu<sub>4</sub>Tyr. KIT reactions contained 1 nM KIT, 50  $\mu$ M ATP, and 100  $\mu$ g/ml poly Glu<sub>4</sub>Tyr. PDGFR- $\beta$  reactions contained 12 nM PDGFR- $\beta$ , 10  $\mu$ M ATP, and 10  $\mu$ g/ml poly Glu<sub>4</sub>Tyr. Typical between-run coefficient of variation was less than 30%.
14. Turner, J. A. *J. Org. Chem.* **1990**, *55*, 4744.
15. Nahm, S.; Weinreb, S. M. *Tetrahedron Lett.* **1981**, *22*, 3815.
16. Garuti, L.; Giovanninetti, G.; Bova, S.; Chiarini, A. *Arch. Pharm.* **1988**, *321*, 377.
17. Varchi, G.; Jensen, A. E.; Dohle, W.; Ricci, A.; Cahiez, G.; Knochel, P. *Synlett* **2001**, 477.
18. Abarbri, M.; Thibonnet, J.; Berillon, L.; Dehmel, F.; Rottlander, M.; Knochel, P. *J. Org. Chem.* **2000**, *65*, 4618.
19. Male B6C3F1 mice (Taconic Farms), 6 weeks of age, were used to define the pharmacodynamic activity of FMS inhibitors. Six hours following an oral dose of vehicle or compound formulated in 20% 2-hydroxypropyl- $\beta$ -cyclodextrin (HPCD), groups of six mice were administered saline or 1.0  $\mu$ g CSF-1 (Cell Biosciences) by tail vein injection. Fifteen minutes later, mice were euthanized. Spleens were isolated and snap frozen on dry ice. The frozen tissue was homogenized in 1 ml of Trizol (Invitrogen) per 50 mg of tissue using a hand-held Pellet Pestle (Kontes). RNA was purified according to the Trizol instructions and treated with 6.8 Kunitz units of RNase free DNase (Qiagen) to degrade contaminating genomic DNA. Sample RNA was purified further using RNeasy columns (Qiagen). RT-PCRs were performed in a 25  $\mu$ L reaction volume using Reverse Transcriptase qPCR Master Mix (Eurogentec) and approximately 50 ng RNA based on OD<sub>260</sub>. Applied Biosystems, Inc., was the source for the primer probe set for mouse c-fos mRNA (part# Mm00487425) and 18S rRNA (part# 4333760F). Amplification and detection were performed using the ABI Prism 7700 Sequence Detection system with the following profile: 48 °C for 30 min, 95 °C for 10 min and 40 cycles of 95 °C for 15 s and 60 °C for 1 min. Standard curves (six 4-fold dilutions) were created for c-fos mRNA and for 18S rRNA using RNA isolated from one vehicle-treated, CSF-1-induced mouse. Relative expression levels in all other samples were calculated based on the standard curves. c-Fos mRNA values were divided by 18S rRNA values to normalize for total RNA content.